MATHEMATICAL BIOSCIENCES
AND ENGINEERING
Volume **13**, Number **3**, June **2016**

doi:10.3934/mbe.2016009

pp. **579–596**

ON THE PROPERTIES OF INPUT-TO-OUTPUT TRANSFORMATIONS IN NEURONAL NETWORKS

Andrey Olypher

School of Science and Technology
Georgia Gwinnett College
Lawrenceville, GA 30043, USA

Jean Vaillant

Department of Mathematics and Informatics
Université des Antilles
Pointe-à-Pitre, Guadeloupe, France

Abstract. Information processing in neuronal networks in certain important cases can be considered as maps of binary vectors, where ones (spikes) and zeros (no spikes) of input neurons are transformed into spikes and no spikes of output neurons. A simple but fundamental characteristic of such a map is how it transforms distances between input vectors into distances between output vectors. We advanced earlier known results by finding an exact solution to this problem for McCulloch-Pitts neurons. The obtained explicit formulas allow for detailed analysis of how the network connectivity and neuronal excitability affect the transformation of distances in neurons. As an application, we explored a simple model of information processing in the hippocampus, a brain area critically implicated in learning and memory. We found network connectivity and neuronal excitability parameter values that optimize discrimination between similar and distinct inputs. A decrease of neuronal excitability, which in biological neurons may be associated with decreased inhibition, impaired the optimality of discrimination.

1. **Introduction.** In many brain areas neuronal spiking does not correlate directly with external stimuli or motor activity of the animal. Neurons transform apparently abstract inputs to abstract outputs. The hippocampus – a brain area critically implicated in learning and memory – provides an important example [1]. Hippocampal principal neurons are connected with tens of thousands input neurons [26]. However, the content of these inputs and corresponding outputs is poorly understood even in the case of the most studied place cells that receive and signal not just the information about the animal's location [14, 28, 27, 7]. Other examples that attracted considerable attention of neuroscientists include the information transfer from the hippocampus to the cortex [37] and from the antennal lobe to the mushroom body in the olfactory system of insects [15, 17].

Analysis of neuronal responses to arbitrary inputs is challenging. Current experimental techniques have limited possibilities. In the hippocampus, the most advanced methods allow for selective activation of no more than hundred synaptic

2010 *Mathematics Subject Classification.* Primary: 92B20, 68T10; Secondary: 68M10, 05D40.
Key words and phrases. Information processing, pattern discrimination, neuronal networks, hippocampus, McCulloch-Pitts neurons.

connections of a principal neuron [21]. In computational models, arbitrary spatio-temporal input patterns can be simulated [22, 12]. However computational resources limit sampling, repertoire and accuracy of the obtained results.

Here we study a special case when information processing in neuronal networks can be considered as maps of binary vectors, where ones (spikes) and zeros (no spikes) of input neurons are transformed into spikes and no spikes of output neurons. Such situations arise when neuronal excitability undergoes strong and fast periodic modulation. Two examples. In behaving rats, neuronal excitability of hippocampal neurons exhibits synchronous oscillations with a 40-100 Hz frequency [4]. In insects, excitability of mushroom body neurons is synchronized at about 50 Hz [33]. What would be the use of a one layer network that recodes its inputs? With regards to the hippocampal field CA1 one hypothesis suggests that CA1 principal cells may recode time-contingent combinations of stimuli, represented in the downstream CA3 network, into more compact representations. For example, simultaneously active representations of stimuli A, B, C, D, and E could be recoded into representations of ABC and BDE [36].

An important and interesting question regarding input-to-output maps in neuronal networks is to how they transform the distances between inputs into the distances between the corresponding outputs (Fig. 1). On one side, the transformation of distances is a fundamental mathematical characteristic of a map. On the other side, it allows one, for example, to contrast normal and abnormal information processing in neuronal networks. Indeed, intuitively, if an input pattern makes a target neuron spike then the 'healthy' target neuron should also spike in response to similar patterns - otherwise, neurons would be too sensitive to noise. At the same time neurons should discriminate between sufficiently different input patterns and spike selectively. In the simple example above, the CA1 network may recode the combination of stimuli A, B, and C and the combination of stimuli A, B, and E similarly or differently. What does determine that?

In [29, 30], we studied this problem using simulations of multi-compartmental models of hippocampal neurons. To proceed with computationally demanding studies of how neuronal excitability and network connectivity affect information processing we needed a deeper understanding of the mathematical properties of the problem, which has led to the study reported here.

Using a combinatorial approach we obtained new results to this problem – exact and explicit formulas for the expected distance between the neuronal outputs provided certain distance between its inputs. These results allow for studying how different input-to-output transformations are for similar and distinct inputs.

The outline of the paper is as follows. Section 2 contains necessary notations and some auxiliary results. We solve the problem in the case when the target neuron is connected with all the neurons of the input network in section 3. This result is used in section 4 to solve the general case in which some neurons of the input network are not connected to the target neuron. Finally, in section 5, we apply the formulas from section 4 to a simple model of a hippocampal network to show how connectivity and excitability of the neuron can optimize the network ability to discriminate between similar and distinct inputs.

Portions of this work were presented in preliminary form in [31].

2. **Definitions and auxiliary results.**

Let $V^n = \{0,1\}^n$ be the space of binary inputs. The components of the binary vectors from V^n equal to one (zero) represent

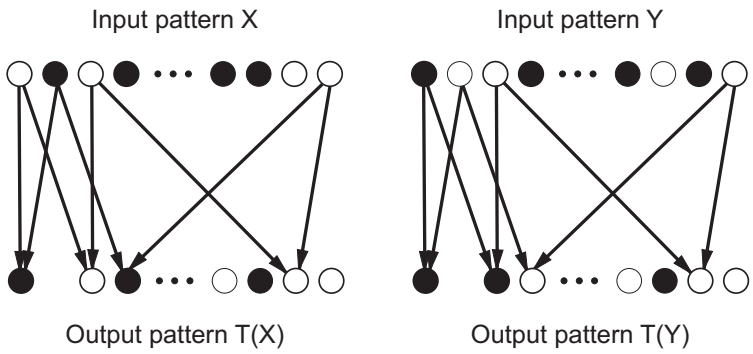

FIGURE 1. Transformation of inputs in a neuronal network. The input pattern is a binary vector that represents activity in input neurons (top circles) within a short time window. Ones in this vector correspond to spiking neurons (filled circles), zeros – to the neurons that do not spike (empty circles). Input neurons are connected to the neurons of the output network (bottom circles). Each input pattern makes some of the output neurons spike. Given the distance between the two input patterns X and Y how close are the output binary patterns T(X) and T(Y)?

spiking (quiescence) of the corresponding input neurons. McCulloch-Pitts (MCP) neurons are binary linear threshold functions on vectors from V^n [25]. Let $L = L(x)$ be such a function. An input $x \in V^n$ makes the MCP neuron spike or $L(x) = 1$, if $\langle w, x\rangle > \theta$; here $\langle w, x\rangle = w_1x_1 + w_2x_2 + \cdots + w_nx_n$ is the dot product of w and x. The neuron is quiescent or $L(x) = 0$ if $\langle w, x\rangle \le \theta$. In what follows we assume that all the components of w are binary, $w \in V^n$.

We studied how input-to-output transformations in MCP neurons depend on the threshold θ, the number n of neurons in the input network, the number m of the input neurons that spike within a time window considered, and the number k of the connections between the output neuron and the input neurons. We assumed that in each input pattern, m simultaneously spiking neurons are selected randomly, the spiking of one input neuron is independent from the spiking of the others, and the patterns are equiprobable. If p – the probability of input neuron spiking, determined by a given mean firing rate, is the same for all the input neurons, then m is equal to the mean number of simultaneously spiking neurons, np. k connections between the target neuron and the input neurons with non-zero weights are randomly distributed and there is no link between the input patterns and the set of non-zero weights. Note that the assumption of random weights does not imply that neurons close to the target neuron cannot have connections with input neurons close to the input neurons of the target neurons (cf. [5]).

By choosing a proper value of the spike threshold θ the input-output curve of the MCP neuron can be made close to the input-output curves of detailed neuronal models. For comparison, we chose a model from [19]. In that model, the principal cell has $k = 4407$ excitatory synapses from CA3 principal cells. The number 4407 was obtained using the estimates of the synaptic densities from [26]. In [30], we reasoned that these synapses could come from a subpopulation of $n = 28009$ CA3 principal cells. To match a typical level of spiking activity in CA3, the number m of spiking CA3 neurons in each random input pattern, a binary vector of length 28009,

was set to 1540. Each excitatory input in the Jarsky et al. (2005) model considered here was accompanied by activation of 871 randomly selected inhibitory synapses. These numbers of the model are of course random samples from the corresponding ranges of feasible values; see discussion of parameter values in [30].

The spike threshold of the MCP neuron was chosen to be $\theta = 258$ to attain the best match between the input-output characteristics of the two neuronal models for $m = 1540$ (Fig. 2).

The input-output characteristic for the MCP neuron in Figure 2 was calculated using the formula

$$Prob(L(x) = 1) = 1 - \sum_{j=0}^{min(k,\theta,m)} \frac{\binom{m}{j}\binom{n-m}{k-j}}{\binom{n}{k}}. \tag{1}$$

The sum in (1) is the probability of not spiking. Each term in the sum is equal to the probability that a weighted combination of the input pattern components is below the threshold θ. The probabilities obey the hypergeometric distribution with parameters n, m, and k.

We characterize the input-to-output transformation in MCP neurons in terms of Hamming distances. The Hamming distance between $x, y \in V^n$ is $H(x, y) = \langle x - y, x - y\rangle$, $0 \le H(x, y) \le n$. The number of ones is the Hamming length $|x|$ of x, $|x| = \sum_{i=1}^{n} x_i = \langle x, x\rangle$. Let V_m^n, $0 \le m \le n$ be the subset of V^n vectors with Hamming length m : $V_m^n = \{x \in V^n, |x| = m\}$.

It is easy to verify that for $x, y \in V_m^n$, $H(x, y)$ obeys a binomial distribution. Indeed, the probability that the Hamming distance between a component of one vector and the correspondent component of the other vector equal one is equal to $2m/n \cdot (1 - m/n)$. Therefore

$$E(H(x, y)) = 2m \cdot (1 - \frac{m}{n}). \tag{2}$$

The maximum of $E(H(x, y))$ is attained at $m = n/2$.

The expected Hamming distance between network outputs is the sum of the expected Hamming distances for individual neurons. Suppose there are N output neurons. Let P_ω be the probability of an input pair ω. Then the Hamming distance between the corresponding outputs for the $i-$th neuron, $H^i(\omega)$, $i = 1, \cdots, N$, is a random variable with the expected value

$$E(H^i) = \sum_{\omega} P_\omega H^i(\omega).$$

Consider now the Hamming distance between the outputs of the whole network $H_{netw} = \sum_{i=1}^{N} H^i$. By definition of the expected value,

$$\hat{H}_{netw} \equiv E(H_{netw}) = \sum_{i=1}^{N} E(H^i). \tag{3}$$

In the case of identical neurons with the same number of connections all $E(H^i)$ are equal, $E(H^i) = \hat{H}$, and $\hat{H}_{netw} = N \cdot \hat{H}$. A trivial generalization holds for networks that consist of several categories of identical neurons. In that case the expected Hamming distance between the outputs of the network is equal to the sum of the products of the expected Hamming distances for individual neurons from the categories and the numbers of neurons in those categories.

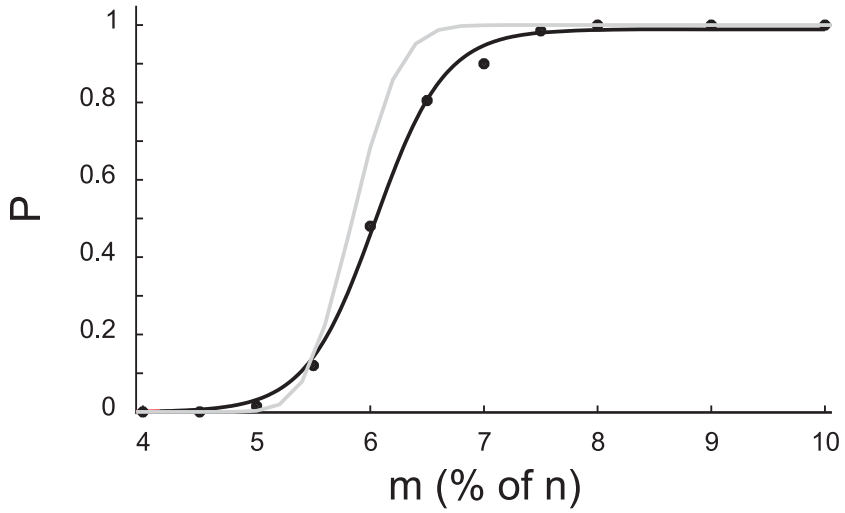

FIGURE 2. Probability of spiking in a detailed model of a hippocampal neuron and an MCP neuron. The hippocampal model neuron and MCP neuron were connected with $k = 4407$ out of $n = 28009$ neurons in the input network. The network had $m\%$ of neurons active. The data points for the probability P of spiking for the detailed neuronal model (dots) are the averages for 200 random input patterns. The points are fitted with a Boltzmann function $a/(1 + exp(-bx + c)) + d$ with $a = -1.004$, $b = 3.161$, $c = -19.98$, $d = 0.9902$ (black curve). For the MCP neuron, P was calculated according to (1) (grey curve). The neuronal model is from [19].

Figure 3 illustrates formula (3) for the case of five input neurons and several ($N = 1, 2, 3$) identical neurons in the output network. For one output MCP neuron $\hat{H} = 0.4$; see (12) below. The figure shows convergence of $\hat{H}_{netw}$ to 0.4, 0.8 and 1.2 for one, two, and three output neurons with the increase of the number of sampled pairs of inputs.

The example of Figure 3 also exposes the lack of independence of output neurons. In the case of independence, H_{netw} for $N = 3$ would obey the binomial distribution with the parameters $N = 3$ and $p = 0.4$. The probabilities of $H_{netw} = 0$, 1, 2, and 3 would be 0.216, 0.432, 0.288, and 0.064 respectively. However, direct evaluation of the probabilities based on the Hamming distances for all 60 possible input pairs gives the values 0.133, 0.600, 0.200, and 0.067.

3. **Uniform binary weighing.** In this section, we consider an auxiliary case when all the synaptic weights of the target neuron are equal to one. Suppose an input x makes the neuron spike. Let Prob $(L(y) = 1 \,|\, L(x) = 1, H(x, y) = d)$ be the probability that an input y makes the MCP neuron spike provided y is at the Hamming distance d from x. This probability characterizes the sensitivity of the neuron L to differences between inputs.

To calculate the probability consider function $f(n, m, m', d)$ equal to the number of the pairs (x, y), $x \in V^n_m$, $y \in V^n_{m'}$, at distance d from each other. A direct counting of the appropriate pairs gives

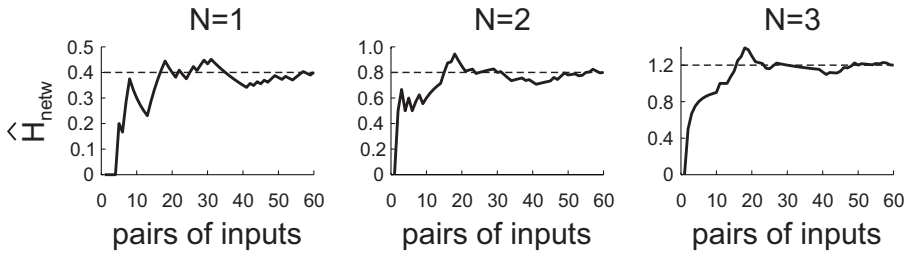

FIGURE 3. Average Hamming distance between outputs of networks. The output networks consisted of one (left), two (middle), and three (right) McCulloch-Pitts neurons with $\theta = 1$. Every output neuron was connected with three ($k = 3$) randomly chosen input neurons. The first neuron was connected with neurons number 1, 3, 4 of the input network. The second and third neurons were connected with the input neurons number 1, 2, 3, and number 2, 3, 5 respectively. The curves represent the average Hamming distance $\hat{H}_{netw}$ across the pairs of 5-dimensional ($n = 5$) input binary vectors with two ones ($m = 2$) in each vector and Hamming distance 2 between them ($d = 2$). The pairs of inputs were selected in random order, the same for the all three graphs. The number of all such pairs is equal to 60. The exact values of $\hat{H}_{netw}$ (dashed lines) are multiples of 0.4, the $\hat{H}_{netw}$ value for one output neuron; see Eqn. (12). n, k, m, d are the parameters of the studied model.

$$\begin{aligned} f(n,m,m',d) &= \binom{n}{m}\binom{m}{\langle x,y\rangle}\binom{n-m}{m'-\langle x,y\rangle} \\ &= \binom{n}{m}\binom{m}{0.5(m+m'-d)}\binom{n-m}{0.5(m'-m+d)}. \end{aligned} \tag{4}$$

In the above formula, $\langle x,y\rangle = 0.5(m+m'-d)$ and $m' - \langle x,y\rangle = 0.5(m'-m+d)$ because of the assumption $H(x,y) = \langle x-y, x-y\rangle = d$.

Using $f(n,m,m',d)$ one can easily obtain the probability mass function of H for $x, y \in V_m^n$ (see also a related result in Appendix.)

Result 1: Suppose $x, y \in V_m^n$. Then

$$Prob(H(x,y) = d) = \frac{\binom{m}{\frac{d}{2}}\binom{n-m}{\frac{d}{2}}}{\binom{n}{m}}. \tag{5}$$

The proof of Result 1 is as follows: formula (5) is the ratio of the number of combinations of $x, y \in V_m^n$ such that $H(x,y) = d$, and the total number of combinations of $x, y \in V_m^n$. The first number is given by $f(n,m,m,d)$. The second number is equal to $\binom{n}{m}^2$. Obvious simplifications lead to the result.

One can verify that the formula (5) is consistent with (2).

Function $f(n,m,m',d)$ can be also interpreted as the number of ways of putting n pairs of vector components (x_i, y_i), $i = 1, \ldots, n$, into 4 distinct categories: $(1,1)$, $(1,0)$, $(0,1)$, and $(0,0)$. Indeed, the expanding of the binomial coefficients in (4) shows that $f(n,m,m',d)$ is the multinomial coefficient

$$f(n,m,m',d)=\frac{n!}{\langle x,y\rangle!(m-\langle x,y\rangle)!(m'-\langle x,y\rangle)!(n-m-m'+\langle x,y\rangle)!}. \tag{6}$$

The main auxiliary result determines the conditional probability that input y makes the neuron L spike provided all the synaptic weights are equal to one ('uniform weighing') and y is at distance d from some input x of length m.

Result 2 : Let $|w|=n$ and $P_u \equiv Prob(L(y)=1 \mid H(x,y)=d,|x|=m)$. Then

$$P_u=\frac{\sum\limits_{m'\in D_{[\theta+1,n]}} f(n,m,m',d)}{\sum\limits_{m'\in D_{[0,n]}} f(n,m,m',d)}, \tag{7}$$

where $D_{[a,b]}$ is the set of all m' from $[a,b]$ such that: 1) $m+m'-d$ is an even number, and 2) $max(d-m,m-d)\le m'\le min(m+d,2n-m-d)$.

Denominator in (7) is the number of all possible combinations of x, $|x|=m$, and y such that $H(x,y)=d$. Numerator is the number of those combinations that satisfy an additional condition $\langle w,y\rangle=|y|=m'>\theta$. The conditions for $D_{[a,b]}$ are those for which all binomial coefficients that involve m' in the corresponding sums have non-negative integer coefficients.

In appendix, we deduce an equivalent form of (7).

To numerically evaluate formulas for probabilities we used Matlab (MathWorks, Natick, MA) and a PC with a 1.5 GHz processor and 2.5 Gb memory. To preserve accuracy, we made calculations with all the digits utilizing a publicly available Matlab package VPI by John D'Errico.

4. Arbitrary binary weighing.

Here we generalize the results of the previous section to the case of arbitrary binary weighing when the target neuron may be not connected with some neurons from the input network. Zero weights can for example model 'silent', ineffective synapses [20]. Silent synapses can be essential for optimal information processing in neurons. For example modelling studies [6, 10] suggest that the maximal storage capacity of Purkinje cells of the cerebellum is attained when a large fraction of their synapses have zero weights.

Below we assume that the non-zero weights are the first k weights of w: $w_i=1$, $i\le k$, $w_i=0$, $i>k$. There is no loss of generality in this assumption since we average across inputs. Let P_k be the projector to the first k coordinates such that $P_kx=(x_1,x_2,\dots,x_k,0,\dots,0)$. Denote $\mu=\langle P_kx,P_kx\rangle$, $\mu'=\langle P_ky,P_ky\rangle$, and $\delta=H(P_kx,P_ky)$. The following proposition determines the probability that input y makes the neuron spike provided input x, $|x|=m$, makes the neuron spike, and $H(x,y)=d$.

Result 3 : Let $|w|=k$, $k\le n$, and let $P_a \equiv Prob(L(y)=1 \mid L(x)=1,H(x,y)=d,|x|=m)$. Then

$$P_a=\frac{\sum\limits_{\delta=0}^{min(d,k)}\sum\limits_{\mu=\lfloor\theta\rfloor+1}^{min(m,k)}\sum\limits_{m'=0}^{n}\sum\limits_{\mu'\in Q_{[\theta+1,m']}} f(k,\mu,\mu',\delta)f(n-k,m-\mu,m'-\mu',d-\delta)}{\sum\limits_{\delta=0}^{min(d,k)}\sum\limits_{\mu=\lfloor\theta\rfloor+1}^{min(m,k)}\sum\limits_{m'=0}^{n}\sum\limits_{\mu'\in Q_{[0,m']}} f(k,\mu,\mu',\delta)f(n-k,m-\mu,m'-\mu',d-\delta)}, \tag{8}$$

where f is defined by formula (4), $\lfloor\theta\rfloor$ is the largest integer not greater than θ, and $Q_{[a,b]}$ is the set of μ' from $[a,b]$ for which all binomial coefficients that involve μ' in the corresponding sum have non-negative integer coefficients.

Let $k < n$. To derive (8) consider first k components of vectors x and y separately from the rest $n-k$ components. For the first k components we can assume that all the weights of L are equal to one. Therefore the number of all the combinations of $P_k x$ and $P_k y$ such that $\langle P_k x, P_k x\rangle = \mu$, $\langle P_k y, P_k y\rangle = \mu'$ and $H(P_k x, P_k y) = \delta$ is equal to $f(k,\mu,\mu',\delta)$; cf. (4). Each of these combinations is multiplied by the number of possible combinations of the rest $n-k$ components. For the latter combinations the weights of L also can be considered uniform (all equal to zero). The number of combinations is also given by function f from (4) with appropriate arguments. Subsets $Q_{[a,b]}$ are natural generalizations of subsets $D_{[a,b]}$ from Result 2. They specify values of μ' from intervals $[a,b]$ such that all binomial coefficients involving μ' in the corresponding sums have non-negative integer lower indexes.

When $k = n$, formula (8) reduces to formula (7). Indeed, δ takes only one value $\delta = d$ provided $m = \mu$ and $m' = \mu'$. Then $f(n-k, m-\mu, m'-\mu', d-\delta) = 1$.

When the inputs have the same length, $m' = m$, formula (8) gets simpler:

$$P_a = \frac{\displaystyle\sum_{\delta=0}^{min(d,k)} \sum_{\mu=\lfloor\theta\rfloor+1}^{min(m,k)} \sum_{\mu'\in Q_{[\theta+1,m]}} f(k,\mu,\mu',\delta) f(n-k, m-\mu, m-\mu', d-\delta)}{\displaystyle\sum_{\delta=0}^{min(d,k)} \sum_{\mu=\lfloor\theta\rfloor+1}^{min(m,k)} \sum_{\mu'\in Q_{[0,m]}} f(k,\mu,\mu',\delta) f(n-k, m-\mu, m-\mu', d-\delta)}. \quad (9)$$

The probability P_a^0 that $L(y) = 0$ provided $|x| = |y| = m$, $L(x) = 0$ and $H(x,y) = d$ can be expressed in a similar way:

$$P_a^0 = \frac{\displaystyle\sum_{\delta=0}^{min(d,k)} \sum_{\mu=0}^{\lfloor\theta\rfloor} \sum_{\mu'\in Q_{[0,\theta]}} f(k,\mu,\mu',\delta) f(n-k, m-\mu, m-\mu', d-\delta)}{\displaystyle\sum_{\delta=0}^{min(d,k)} \sum_{\mu=0}^{\lfloor\theta\rfloor} \sum_{\mu'\in Q_{[0,m]}} f(k,\mu,\mu',\delta) f(n-k, m-\mu, m-\mu', d-\delta)}. \quad (10)$$

From Result 3, we get the following result which determines the probability that two binary inputs x and y of length d, that make the neuron spike, are at Hamming distance d from each other.

Result 4 : Let $|w| = k$, $k \le n$, $|x| = |y| = m$. Then

$$Prob(H(x,y) = d \mid L(x) = 1, L(y) = 1)$$

$$= \frac{\displaystyle\sum_{\delta=0}^{min(d,k)} \sum_{\mu=\lfloor\theta\rfloor+1}^{min(m,k)} \sum_{\mu'\in Q_{[\theta+1,m']}} f(k,\mu,\mu',\delta) f(n-k, m-\mu, m-\mu', d-\delta)}{\left(\displaystyle\sum_{\mu=\lfloor\theta\rfloor+1}^{min(m,k)} \binom{m}{\mu}\binom{n-m}{k-\mu}\right)^2}. \quad (11)$$

The numerator in (11) is the same as in formula (9) and the denominator is the total number of combinations of $x, y \in V_m^n$ such that $L(x) = L(y) = 1$ for the case $k \le n$.

Using the above results we now obtain a formula for the expected Hamming distance $\hat{H}$ between $L(x)$ and $L(y)$ provided x and y have the same Hamming length m and are at Hamming distance d from each other. $\hat{H}$ close to one implies neuron L has often the same value on two input patterns x and y. $\hat{H}$ close to zero implies neuron L has often different values on two input patterns x and y.

Result 5 : Let $x, y \in V_m^n$, $H(x,y) = d$ and L is a neuron with the weights $w \in V_k^n$. Then $\hat{H}$, the expected Hamming distance between $L(x)$ and $L(y)$, is equal to

$$\hat{H} = 1 - (P_a \cdot Prob(L(x) = 1) + P_a^0 \cdot Prob(L(x) = 0)). \tag{12}$$

In (12), P_a is determined by (9), P_a^0 by (10), and $Prob(L(x) = 1)$ by (1); $Prob(L(x) = 0) = 1 - Prob(L(x) = 1)$.

Note that in the case when all the weights are equal to one, $|w| = n$, $\hat{H} \equiv 0$. If $m > \theta$ then $H(L(x), L(y)) = 0$ since $L(x) = 1$ and $L(y) = 1$. If $m \leq \theta$ then $H(L(x), L(y)) = 0$ since $L(x) = 0$ and $L(y) = 0$.

To approximate function f (Eqn. (6)) one can use the Stirling's formula for factorials ([13], p.54) according to which for any natural n

$$n! \approx \sqrt{2\pi} n^{n+0.5} e^{-n} \big(1 + \frac{1}{12n}\big). \tag{13}$$

The next section has an example of using such an appoximation.

5. **Application.** We applied the above formulas to analyze information processing in the field CA1 principal cells of the rat hippocampus during slow gamma (25-55Hz) populational rhythm when the input to CA1 is predominantly formed by inputs from CA3 neurons [3]. In the context of our model, inhibitory interneurons of the CA1 network contribute to input-to-output transformation in CA1 principal cells in two ways. Feed-forward interneurons mostly determine the value of the threshold θ. Feed-back interneurons help to synchronize and discretize excitability in principal cells. They also reset the excitability by the beginning of every input-to-output cycle of transformation. The MCP model obviously does not exhibit any behavior other than spiking or no spiking. Yet, as we showed earlier (Fig. 2), the averaged input-to-output characteristic of the MCP model can be made close to that of a detailed neuronal model which in turn approximates the corresponding properties of biological neurons [19].

In the first example, we adapted the model of a CA1 neuron from [12]. The input network, representing neurons from the field CA3 of the hippocampus, consisted of $n = 100$ neurons. The binary patterns had length $m = 20$. The spike threshold level $\theta = 8$ roughly corresponded to the average level of spiking of the CA1 neurons in the model. We evaluated $\hat{H}$ using (12) for $\theta = 8$ and $\theta = 4$. In accord with intuition, small distances d between x and y were transformed into small expected distances $\hat{H}$ between the corresponding outputs for the both threshold values (Fig. 4). However, for $\theta = 8$ the greatest values of $\hat{H}$ were attained at about two times greater values of k compared to the case $\theta = 4$.

To reveal the difference between the cases of $\theta = 8$ and $\theta = 4$ we looked at the corresponding values of P_a. In both cases, P_a had a qualitatively similar dependence from the number k of unit weights of the neuron and from the distance d between the inputs (Fig. 5A, B). However, for some values of k and d the difference was quite notable (Fig. 5C).

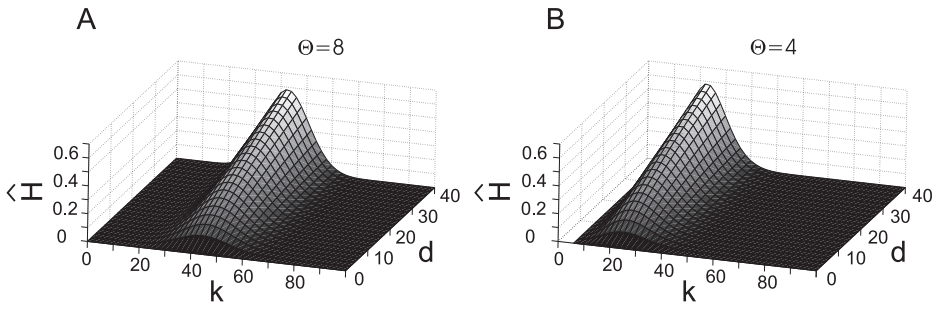

FIGURE 4. Expected Hamming distance $\hat{H}$ between outputs $L(x)$, $L(y)$ of neuron L as a function of the Hamming distance d between inputs x, y and the number of non-zero weights k. (A) $\theta = 8$. (B) $\theta = 4$. $n = 100$, $m = m' = 20$.

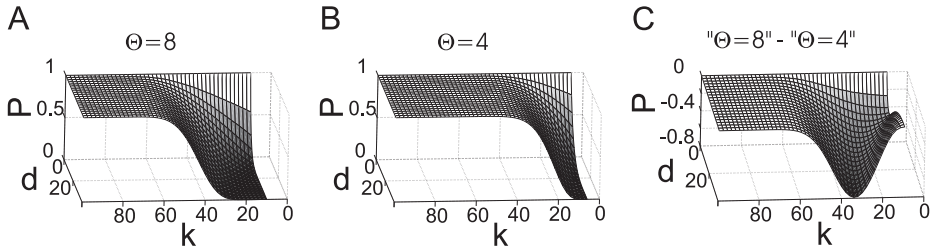

FIGURE 5. Probability that an input makes a neuron spike conditional on proximity to another input that makes the neuron spike. Probability $P \equiv P_a$ as a function of the distance d between inputs and the number k of non-zero weights in the neuron is shown for two different values of threshold θ, (A) $\theta = 8$ and (B) $\theta = 4$. (C) The difference between the probabilities in (A) and (B) is small for most but not all values of k and d. $n = 100$, $m = m' = 20$.

We chose two values of d for the further analysis. One value, $d = 32$, is the expected distance between a pair of randomly selected binary patterns with 20 ones out of 100 (cf. (12)). It is equal to 80% of the maximal distance $d = 40$. We refer to the patterns with such distance between each other as distinct. The other value $d = 4$ is 10% of the maximal distance between patterns. We refer to the patterns with such d as similar.

Figure 6A shows the probability of neuronal spiking for similar (black curve) and distinct (gray curve) patterns. The difference between the probabilities (dotted curve) attained the maximum at $k = 30$, that is when the model CA1 neuron was connected with 30 CA3 neurons. The maximal difference between the probabilities for the two categories of patterns was equal to 0.55.

A decrease of the spiking threshold from $\theta = 8$ to $\theta = 4$ made the connectivity with thirty CA3 input neurons non-optimal (Fig. 6B). The conditional probabilities of spiking for similar and distinct patterns changed, as well as the difference between them. As a result, the difference between the probabilities for $k = 30$ became equal

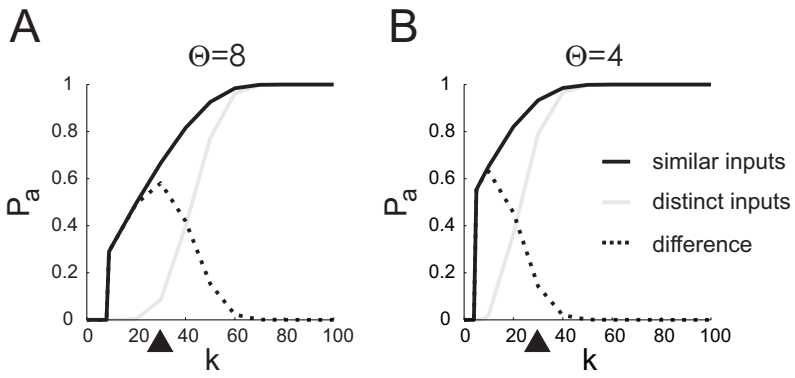

FIGURE 6. Probability of neuronal spiking for distinct and similar inputs. (A) The probability for similar inputs ($d = 4$) (black) and distinct inputs ($d = 32$) (gray) has maximal difference (dotted) for $k = 30$ nonzero weights (black triangle) for $\theta = 8$. (B) For a smaller threshold $\theta = 4$, $k = 30$ does not maximize the difference between the probabilities. $n = 100$, $m = m' = 20$.

to 0.14 that signifies a considerable decrease of the neuron's ability to discriminate between similar and distinct inputs.

We conclude the first example with an application of the Sterling's formula (13) to evaluation of the expected Hamming distance from Fig. 4A. First, we expressed the formula (12) for $\hat{H}$ in terms of function f (Eqn. (6)) :

$$\begin{aligned}\hat{H} = \Big(&\sum_{\delta=0}^{min(d,k)} \sum_{\mu=0}^{min(m,k,\lfloor\theta\rfloor)} \sum_{\mu' \in Q_{[\theta+1,m]}} f(k,\mu,\mu',\delta) f(n-k, m-\mu, m-\mu', d-\delta) \\ &+ \sum_{\mu \in Q_{\lfloor\theta\rfloor+1,m)}}^{min(m,k)} \sum_{\mu'=0}^{min(m,k,\lfloor\theta\rfloor)} f(k,\mu,\mu',\delta) f(n-k, m-\mu, m-\mu', d-\delta)\Big) \\ &* f(n,m,m,d)^{-1}.\end{aligned} \tag{14}$$

The divisor at the very end of the formula stands for the number of pairs (x, y), $x, y \in V_m^n$, such that $H(x, y) = d$. The rest of the formula is the number of $x, y \in V_m^n$ with $H(x, y) = d$ and such that either $L(x) = 0, L(y) = 1$ (first term) or $L(x) = 1, L(y) = 0$ (second term). For multinomial coefficients (cf. (Eqn. (6)) the Sterling's formula implies

$$\begin{aligned}\frac{n!}{x_1!x_2!x_3!x_4!} \approx exp\{&nln(n) + 0.5ln(2\pi n) + ln(1 + 1/(12n)) \\ &- \sum_{i=1}^{4} x_i ln(x_i) + 0.5ln(2\pi x_i) + ln(1 + 1/(12x_i))\}.\end{aligned} \tag{15}$$

Every term in sum (14) consists of a product of two multinomial coefficients divided by another one. For those coefficients we combined the exponents of (15) for computational efficiency.

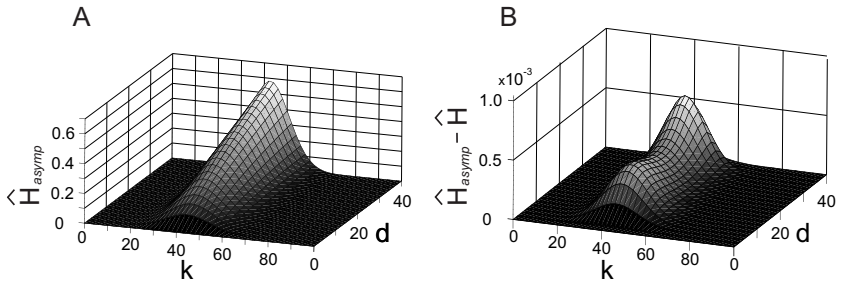

FIGURE 7. The expected Hamming distance $\hat{H}_{asymp}$ between outputs $L(x)$, $L(y)$ of neuron L as a function of the Hamming distance d between inputs x, y and the number of non-zero weights k approximated using the Stirling's formula. (A) $\hat{H}_{asymp}$. (B) $\hat{H}_{asymp} - \hat{H}$, where $\hat{H}$ is the expected Hamming distance calculated 'exactly' (Fig. 4A). $n = 100$, $m = m' = 20$, $\theta = 8$.

The values of $\hat{H}_{asymp}$ obtained using (14), (15) were very close to the exact values of $\hat{H}$ (Fig. 7A). The difference $|\hat{H} - \hat{H}_{asymp}|$ did not exceed 1×10^{-3} (Fig. 7B) and was everywhere negative. Importantly, it took about two orders of magnitude less time to compute $\hat{H}_{asymp}$ than to compute $\hat{H}$. When only the main term of the Sterling's formula (without $1/12n$) was used, the error of the approximation was notably larger, up to 0.06, but the characteristic behavior of $\hat{H}$ was still captured.

In the second example, we considered an MCP neuron, which approximates a multi-compartmental model of a CA1 neuron from [19]. As we mentioned above, the target neuron was connected with $k = 4407$ out of $n = 28009$ CA3 model neurons. The typical level of activity in the network of CA3 neurons corresponded to $m = 1540$. The spike threshold of the MCP neuron was chosen to be $\theta = 258$ to attain the best match between the input-output characteristics of the two neuronal models for that value of m (Fig. 2).

We studied the probability that this model neuron spikes differently to different inputs of fixed Hamming length. We considered $\langle \hat{H} \rangle_d$, the average Hamming distance between the neuronal outputs, equal to $\hat{H}$ additionally averaged with respect to all possible Hamming distances between pairs of inputs.

One way to calculate $\langle \hat{H} \rangle_d$ is to use the formula

$$\langle \hat{H} \rangle_d = \sum_{d=0}^{2m} \hat{H} \cdot Prob(H(x,y) = d)$$

with $\hat{H}$ and $Prob(H(x,y) = d)$ determined by (12) and (5) respectively.

We used a simpler formula

$$\langle \hat{H} \rangle_d = 2 \cdot Prob(L(x) = 1) \cdot (1 - Prob(L(x) = 1)), \tag{16}$$

with $Prob(L(x) = 1)$ determined by (1).

We varied k with step 20 starting from $k = 0$. $\langle \hat{H} \rangle_d$ attained its maximal value at $k = 4700$ (Fig. 8), which is close to $k = 4407$, the number of input connections of the multi-compartmental neuronal model. When the threshold was decreased by 20% to $\theta = 206.4$, the curve for $\langle \hat{H} \rangle_d$ shifted to the left, as in the first example (cf. Fig. 4). The maximum was attained at $k = 3760$.

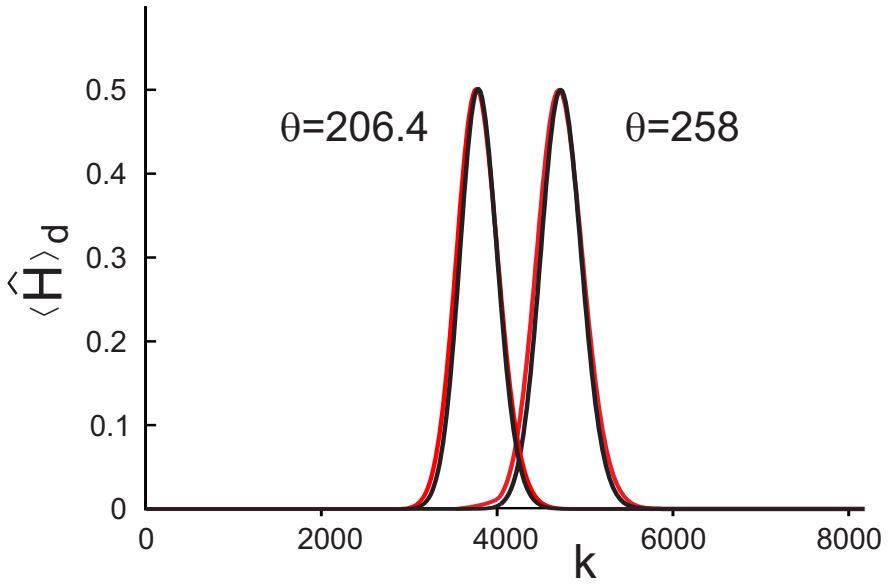

FIGURE 8. Probability of different responses to different inputs in an MCP neuron. $\langle \hat{H} \rangle_d$ from (16) (black curves) as a function of k. When $\theta = 258$ was decreased by 20% to $\theta = 206.4$ the value of k at which $\langle \hat{H} \rangle_d$ attained its maximum decreased from $k = 4700$ to $k = 3760$. Close values of $\langle \hat{H} \rangle_d$ were obtained under the assumption that the number of spikes in the input patterns was not fixed but followed a binomial distribution [15] (red curves); $n = 28009$ and $m = 1550$.

In evaluating $\langle \hat{H} \rangle_d$ one may approximate the probability of neuronal spiking in the input network by m/n as in [15] instead of restricting the number of spiking neurons by m, and correspondingly use not a hypergeometric, as in (1), but a binomial distribution. Both approaches give similar results for the parameters considered (Fig. 8) .

6. **Discussion and conclusions.** One of the basic characteristics of neuronal information processing is how they discriminate inputs. In this work, we modeled the case when the activity of neurons in input and output networks is discretized in time, for example by synchronous periodic modulation of excitability. Then spiking or quiescence of input neurons within a time bin can be considered as an input binary pattern and the resulting spiking of output neurons as the corresponding output binary pattern.

When the distance between pairs of input patterns is fixed, there is a distribution of the distances between pairs of the corresponding output patterns. In the case of one output neuron the distribution is determined by the probability that if an input makes the output neuron spike then another input, at a certain distance from the first one, also makes the output neuron spike. We found an exact and explicit formula for this probability for individual McCallough - Pitts (MCP) neurons.

A natural question regarding input-to-output transformations in neurons is whether these transformations are optimal in processing different inputs. Various criteria of optimality are possible. An earlier result allowed to determine parameters for which the input-to-output transformation in MCP neurons maximally separated different inputs on average [15]. That result applies mostly to pairs of distinct inputs because under the assumption of binomial distribution used in [15] the expected difference between inputs is relatively large (cf. (5)). However, in biological networks many inputs representing the same or similar states of the environment are often similar. The formulas such as the one for $\hat{H}$ (Eqn. 14) can be used for such inputs since these formulas depend on the distance d between input patterns but not on the probability of that.

Here, we focused on transformations of distinct and similar inputs. The analysis of input-to-output transformations between similar and distinct inputs is important since neurons have to be reliable and robust to ignore minor differences between inputs and at the same time be selective to acknowledge major differences between inputs; see also a discussion in [37]. The behavior of the mean distance between neuronal responses as a function of the distance between inputs, when the inputs and responses occur within short time windows, can be used as a quantitative characteristic of neuronal functioning. This characteristic can complement such standard characteristics as for example the input-output characteristic that shows the probability of neuronal spiking in response to neuronal stimulation with certain frequency.

An example, considered in this work, suggests that an optimal discrimination between similar and distinct inputs requires a balance between network connectivity and neuronal excitability. In particular, more excitable neurons should receive inputs from a smaller number of neurons to discriminate between similar and distinct input patterns (Fig. 5 and Fig. 6). Further studies should clarify the nature of this balance.

A difference between a transformation of such inputs was found in a network of multi-compartmental models of CA1 pyramidal neurons [30]. In that model, the connectivity parameter k was about 15 % of the total number of input neurons. Our results (Fig. 5) suggest that such a difference can be a common phenomenon when the proportion of the input neurons that effect the target neuron is relatively small, as in the case of CA1 network.

In the present work we studied how CA1 processed CA3 inputs. In a similar way one can study processing of EC inputs in CA1. A separate analysis of CA3 and EC inputs makes sense since in rats, involved in exploratory behavior, the hippocampal field CA1 neurons tend to process their inputs from another hippocampal field, CA3, and entorhinal cortex (EC) separately in time [11, 3]. The differences in CA1 responses are mostly attributed to the different nature of signals generated by CA3 and EC networks. In particular, the CA3 network, in contrast to the EC network, supposedly follows attractor dynamics [35]. We hypothesize that the CA3 and EC signals are not just different but also CA1 principal cells process the signals from CA3 and EC differently. Namely, CA1 neurons are less sensitive to small variations in CA3 inputs compared to small variations in EC inputs. The network model and the corresponding formulas obtained in the present study suggest focusing on connectivity between CA3, EC and CA1 principal neurons (parameters n and k in the present model) and the level of spiking activity in CA3 and EC (parameter m in the present model) along with the neurophysiological properties of synapses

and the effect of feedforward interneurons (parameter θ in the present model) to verify the reason(s) for different CA1 processing of CA3 and EC inputs. In [30] we proposed that the above hypothesis can be tested experimentally by stimulating CA3 and EC presynaptic sites of CA1 principal cells and comparing variability of CA1 responses. The formulas obtained in the present study should help in designing this experiment and interpreting its results.

Analysis of linear threshold functions has a relatively long history; see, e.g. [9]. Our results are related most closely to the recent results of García-Sánchez and Huerta [15] and Valiant [37], who also studied input-to-output transformations in MCP neurons. Compared to [15], our work is more concerned with specific distances between inputs, rather than just different inputs. Valiant [37] studied input-to-output transformation with a focus on sequences of the corresponding maps and fixed points of those maps.

The MCP neuronal model with binary weights that we used in this study is an oversimplification of a biological neuron. Recent experimental data provide some support to this model. In particular, input-to-output transformations in hippocampal neurons and networks in some cases allow for linear approximation [8, 32]. Next, the assumption of binary synaptic weights is equivalent to the assumption that some synapses are ineffective while the others are of equal weight. In the case of the hippocampal field CA1 the assumption is supported by the observation that excitatory synapses at different locations make similar contribution to the changes of the membrane potential in the soma of the neurons in that area [24, 34]. Ongoing research on hippocampal synapses (see e.g. [2]) should further clarify the accuracy of our assumptions.

The results of our study offer a new approach in experimenting with multiple neuron stimulations. In addition to analyses of neuronal responses to individual input patterns, one can estimate differences between the input patterns and explore the differences between the corresponding output patterns. The results for simple networks of MCP neurons obtained in this study may help in such research.

From the mathematical and computational point of view the results of the present study can be developed in a number of directions. One direction is to design approximations and efficient computational algorithms for numerical evaluation of the formulas. Here, as an example, we demonstrated that using the Sterling's formula for factorials drastically decreased the computation time without considerable loss of accuracy. This approach can be refined further as proposed in ([23, 18]).

Another direction is to take into account small random variations of weights and inputs and use the firing probability of output neurons, conditional on Hamming distance between unperturbed pairs of inputs, as a sensitivity measure of the impact of such variations on the predicted firing.

Acknowledgments. The author thank the anonymous reviewers for their valuable comments. The study was supported in part by the Bonus Qualité Recherche from the UAG Scientific Council.

Appendix. Here we simplify (7) using some properties of binomial coefficients. We rewrite (7) using the definition (4) of the function $f(n, m, m', d)$. The coefficient $\binom{n}{m}$ in numerator and denominator of the formula can be canceled out. Denominator

$$S = \sum_{m'=0}^{n} \binom{m}{0.5(m+m'-d)} \binom{n-m}{0.5(m'-m+d)} \tag{17}$$

$$= \sum_{m'=0}^{n} \binom{m}{0.5(m-d)+0.5m'} \binom{n-m}{0.5(d-m)+0.5m'}$$

can be simplified using a variant of Vandermonde's identity ([16], Eqn.(5.23))

$$\sum_{k} \binom{l}{m+k} \binom{s}{n+k} = \binom{l+s}{l-m+n}, \tag{18}$$

that is valid for nonnegative integer l, and integer m, n. When $m-d$, and consequently m' are both even then the application of (18) to (17) yields $S = \binom{n}{d}$. In the case when $m-d$ is odd m' is also odd, and (18) can be applied to

$$S = \sum_{m'=1}^{n} \binom{m}{0.5(m-d+1)+0.5(m'-1)} \binom{n-m}{0.5(d-m+1)+0.5(m'-1))}.$$

The result is the same, $S = \binom{n}{d}$, and the formula (7) becomes

$$P_u = \frac{\sum_{m'=\theta+1}^{n} \binom{m}{0.5(m+m'-d)} \binom{n-m}{0.5(m'-m+d)}}{\binom{n}{d}}. \tag{19}$$

The symmetry relation $\binom{n}{k} = \binom{n}{n-k}$ applied to $\binom{m}{0.5(m+m'-d)}$, turns formula (19) into a sum of the probabilities of the hypergeometric distribution with parameters n, m, d:

$$P_u = \sum_{m'=\theta+1}^{n} \frac{\binom{m}{0.5(m-m'+d)} \binom{n-m}{0.5(m'-m+d)}}{\binom{n}{d}}. \tag{20}$$

Formula (20) leads to a formula that quantifies the distribution of binary patterns of fixed Hamming weight.

Result 6 : Let $x \in V_m^n$, $y \in V^n$, and $H(x,y) = d$. Then

$$Prob(y \in V_m^n \mid x \in V_m^n, H(x,y) = d) = \begin{cases} \dfrac{\binom{m}{\frac{d}{2}} \binom{n-m}{\frac{d}{2}}}{\binom{n}{d}} & \text{if} \quad \dfrac{d}{2} \le m \le n - \dfrac{d}{2}, \\ 0 & \text{otherwise.} \end{cases}$$

To prove Result 6, in (20) choose θ so that $m > \theta$. For $m' = m$, the sum in (20) reduces just to one term. Inequalities in Result 6 follow from the condition that the low values in the binomial coefficients are non-negative integers.

Figure 9 represents the probabilities from Result 6 calculated for $n = 20000$ (a typical number of inputs to a cortical neuron) depending on the number m of ones (activated synapses) in the pattern and Hamming distance d. Note that the curves do not represent probability density functions. For $d = 0$, $x = y$ the curve is the horizontal line $Prob = 1$. The probability from Result 6 is symmetric about $m = n/2$ and attains its maximum at this value. Indeed, according to an urn model for the hypergeometric distribution, the calculated probability is the probability of having an equal number of black and white balls in a sample of d balls picked at random from an urn that has m black and $n - m$ white balls. Accordingly, the

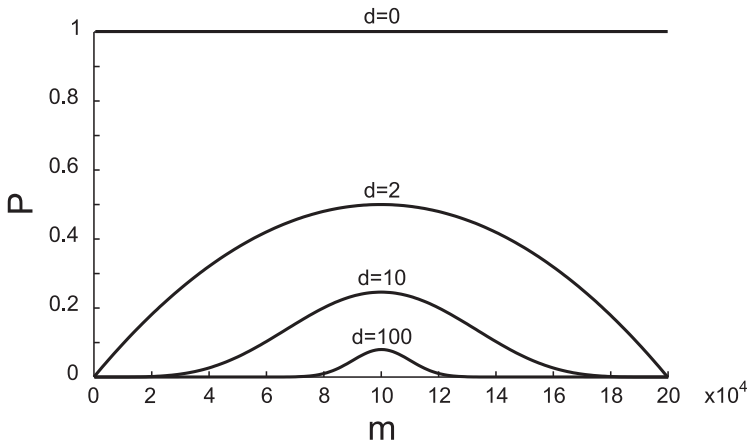

FIGURE 9. Probability that binary vectors have the same Hamming length provided certain distance between them. P is the probability that the binary vector y has the Hamming weight m provided $H(x,y) = d$ and $|x| = m$. $n = 20000$.

probability is the greatest when the number of black and white balls is the same, $m = n/2$ (for even n) or differs by one (for odd n).

REFERENCES

[1] P. Andersen, R. Morris, D. Amaral T. Bliss and J. O'Keefe, Historical perspective: Proposed functions, biological characteristics, and neurobiological models of the hippocampus, in *The Hippocampus Book* (eds. P. Andersen, R. Morris, D. Amaral, T. Bliss and J. O'Keefe), Oxford University Press, 2006, 9–36.

[2] T. M. Bartol, C. Bromer, J. Kinney, M. A. Chirillo, J. N. Bourne, K. M. Harris and T. J. Sejnowski, Hippocampal spine head sizes are highly precise, preprint, (2015).

[3] K. W. Bieri, K. N. Bobbitt and L. L. Colgin, Slow and fast gamma rhythms coordinate different spatial coding modes in hippocampal place cells, *Neuron*, **82** (2014), 670–681.

[4] A. Bragin, G. Jando, Z. Nadasdy, J. Hetke, K. Wise and G. Buzsaki, Gamma (40-100 Hz) oscillation in the hippocampus of the behaving rat, *J. Neurosci.*, **15** (1995), 47–60.

[5] I. H. Brivanlou, J. L. Dantzker, C. F. Stevens and E. M. Callaway, Topographic specificity of functional connections from hippocampal CA3 to CA1, *Proc. Natl. Acad. Sci. USA*, **101** (2004), 2560–2565.

[6] N. Brunel, V. Hakim, P. Isope, J. P. Nadal and B. Barbour, Optimal information storage and the distribution of synaptic weights: Perceptron versus Purkinje cell, *Neuron*, **43** (2004), 745–757.

[7] D. Bush, C. Barry and N. Burgess, What do grid cells contribute to place cell firing? *Trends Neurosci.*, **37** (2014), 136–145.

[8] S. Cash and R. Yuste, Linear summation of excitatory inputs by CA1 pyramidal neurons, *Neuron*, **22** (1999), 383–394.

[9] C. K. Chow, On the characterization of threshold functions, *Proc. Symposium on Switching Circuit Theory and Logical Design (FOCS),* (1961), 34–38.

[10] C. Clopath and N. Brunel, Optimal properties of analog perceptrons with excitatory weights, *PLoS Comput. Biol.*, **9** (2013), e1002919.

[11] L. L. Colgin and E. I. Moser, Gamma oscillations in the hippocampus, *Physiology (Bethesda)*, **25** (2010), 319–329.

[12] V. Cutsuridis, S. Cobb and B. P. Graham, Encoding and retrieval in a model of the hippocampal CA1 microcircuit, *Hippocampus*, **20** (2010), 423–446.

[13] W. Feller, *An Introduction to Probability Theory and Its Applications,* Wiley, New York, NY, 1968.

[14] A. A. Fenton and R. Muller, Place cell discharge is extremely variable during individual passes of the rat through the firing field, *P. Natl. Acad. Sci. USA*, **95** (1998), 3182–3187.
[15] M. García-Sanchez and R. Huerta, Design parameters of the fan-out phase of sensory systems, *J. Comput. Neurosci.*, **15** (2003), 5–17.
[16] R. L. Graham, D. E. Knuth and O. Patashnik, *Concrete Mathematics: A Foundation for Computer Science,* 2^{nd} edition, Addison-Wesley Professional, 1994.
[17] R. Huerta, Learning pattern recognition and decision making in the insect brain, *Proc. of AIP Conf.*, **1510** (2013), 101–119.
[18] F. Izsák, Maximum likelihood estimation for constrained parameters of multinomial distributions – Application to Zipf-Mandelbrot models, *Comput. Stat. Data Anal.,* **51** (2006), 1575–1583.
[19] T. Jarsky, A. Roxin, W. L. Kath and N. Spruston, Conditional dendritic spike propagation following distal synaptic activation of hippocampal CA1 pyramidal neurons, *Nat. Neurosci.*, **8** (2005), 1667–1676.
[20] G. A. Kerchner and R. A. Nicoll, Silent synapses and the emergence of a postsynaptic mechanism for LTP, *Nat. Rev. Neurosci.*, **9** (2008), 813–825.
[21] R. Kramer, D. Fortin and D. Trauner, New photochemical tools for controlling neuronal activity, *Curr. Opin. Neurobiol.*, **19** (2009), 544–552.
[22] X. Li and G. A. Ascoli, Effects of synaptic synchrony on the neuronal input-output relationship, *Neural. Comput.*, **20** (2008), 1717–1731.
[23] C. Loader, Fast and accurate computation of binomial probabilities, 2000. Available from: http://savannah.gnu.org/bugs/download.php?file_id=24016.
[24] J. C. Magee and E. P. Cook, Somatic epsp amplitude is independent of synapse location in hippocampal pyramidal neurons, *Nat. Neurosci.*, **3** (2000), 895–903.
[25] W. McCulloch and W. Pitts, A logical calculus of the ideas immanent in nervous activity, *B. Math. Biophys.*, **5** (1943), 115–133.
[26] M. Megias, Z. Emri, T. F. Freund and A. I. Gulyas, Total number and distribution of inhibitory and excitatory synapses on hippocampal CA1 pyramidal cells, *Neuroscience*, **102** (2001), 527–540.
[27] E. I. Moser and M. B. Moser, Grid cells and neural coding in high-end cortices, *Neuron*, **80** (2013), 765–774.
[28] A. V. Olypher, P. Lansky and A. A. Fenton, Properties of the extra-positional signal in hippocampal place cell discharge derived from the overdispersion in location-specific firing, *Neuroscience*, **111** (2002), 553–566.
[29] A. V. Olypher, W. W. Lytton and A. A. Prinz, Transformation of inputs in a model of the rat hippocampal CA1 network, *SFN Meeting Planner*, **11** (2010), p56.
[30] A. V. Olypher, W. W. Lytton and A. A. Prinz, Input-to-output transformation in a model of the rat hippocampal CA1 network, *Front Comput. Neurosci.*, **6** (2012), p57.
[31] A. Olypher and J. Vaillant, On the properties of input-to-output transformations in networks of perceptrons, arXiv:1312.1206, (2013).
[32] D. Parameshwaran and U. S. Bhalla, Summation in the hippocampal CA3-CA1 network remains robustly linear following inhibitory modulation and plasticity, but undergoes scaling and offset transformations, *Front Comput. Neurosci.*, **6** (2012), p71.
[33] J. Perez-Orive, O. Mazor, G. C. Turner, S. Cassenaer, R. I. Wilson and G. Laurent, Oscillations and sparsening of odor representations in the mushroom body, *Science*, **297** (2002), 359–365.
[34] M. Smith, G. Ellis-Davies and J. Magee, Mechanism of the distance-dependent scaling of schaffer collateral synapses in rat CA1 pyramidal neurons, *J. Physiol.*, **548** (2003), 245–258.
[35] T. Solstad, H. N. Yousif and T. J. Sejnowski, Place cell rate remapping by CA3 recurrent collaterals, *PLoS Comput. Biol.*, **10** (2014), e1003648.
[36] A. Treves and E. T. Rolls, Computational analysis of the role of the hippocampus in memory, *Hippocampus*, **4** (1994), 374–391.
[37] L. G. Valiant, The hippocampus as a stable memory allocator for cortex, *Neural Comput.*, **24** (2012), 2873–2899.

Received March 04, 2015; Accepted October 19, 2015.

E-mail address: aolifer@ggc.edu
E-mail address: Jean.Vaillant@univ-ag.fr